Deficient TiO_{2-x} Coated Porous SiO Anodes for High-rate Lithium-ion Batteries

Yue Xu, [a] Yang Li, [a] Yong Qian, [b] Shanshan Sun, [c] Ning Lin*[a] and Yitai Qian*[a, b]

[a] *Department of Applied Chemistry, University of Science and Technology of China, Hefei 230026, P. R. China*

[b] *Hefei National Laboratory for Physical Sciences at the Microscale, University of Science and Technology of China, Hefei 230026, P. R. China*

[c] *Ningbo University of Technology, Ningbo 315211, P. R. China*

Corresponding Author:

*E-mail: ningl@mail.ustc.edu.cn; ytqian@ustc.edu.cn

Characterization

The X-ray diffraction spectra (XRD) of samples were performed on a Philips X' Pert X ray diffractometer with Cu Kα (λ=1.5406 Å). Raman spectra were carried out using the JYLABRAM-HR Confocal Laser Micro-Raman spectrometer with the 532 nm excitation light source. The X-ray photoelectron spectroscopy was measured on an ESCALAB 250 X-ray photoelectron spectrometer (Perkin-Elmer). The electron paramagnetic resonance (EPR) signals of solid powders were gathered on a JES-FA200 spectrometer. The scanning electron microscopy (SEM, JEOL-JSM-6700F), transmission electron microscopy (TEM, Hitachi H7650) and high resolution transmission electron microscopy (HRTEM, JEM-2100F) were employed to observe the morphology of samples. The specific surface area and pore size distributions of materials were collected on a BEL SORP-max machine (BEL, Japan).

Electrochemical measurement

The electrochemical performance of pristine SiO, porous SiO and porous SiO/TiO_{2-x} composites were measured by the CR2016 coin-type cell, which was assembled in an argon-filled grove box with the contents of H_2O and O_2 less than 0.1 ppm. The prepared electrode slurry is composed of 80 wt. % active materials, 10 wt. % super P and 10 wt. % carboxymethyl cellulose (CMC) with the addition of certain amount of deionized water. Then, pasting the mixed slurry on a copper foil and dried in a vacuum oven at 100 ℃ for 6 h. The average loading mass of the active materials is about 0.8±0.1 mg cm^{-2}. During the half-cell test process, a pure lithium foil was used as the counter electrode with the configured electrolyte which contains 1 M $LiPF_6$ dissolving in the mixture of ethylenecarbonate (EC)/dimethylcarbonate (DMC) (1:1 in volume), 5 wt. % fluoroethylene carbonate (FEC) and 2 wt.% vinylene carbonate (VC). A CHI 660D Electrochemical Workstation was employed to measure the cyclic voltammogram (CV) and electrochemical impedance spectroscopy (EIS) of samples. Meanwhile, the galvanostatic charge/discharge process under different current densities was performed on LANDCT2001A system with the voltage rage between 0.005 V~ 2.0 V.

For the full-cell testing, the cathode is composed of commercial $LiCoO_2$ (Ningbo Veken Battery Co., Ltd.), super P and polyvinylidene fluoride binder with the weight ratio of 90: 5: 5. Then the prepared slurry is dissolved in certain amounts of N-methyl-2-pyrrolidone solvent and pasted on an Al foil. The average loading mass of the active materials is about 1.0±0.1 mg cm^{-2} and the N/P ratio is about 1.5. The battery assembly process is the same as half-cells. The galvanostatic charge/discharge performance was measured on LANDCT2001A system with the voltage rage between 1.5 V~ 4.3 V.

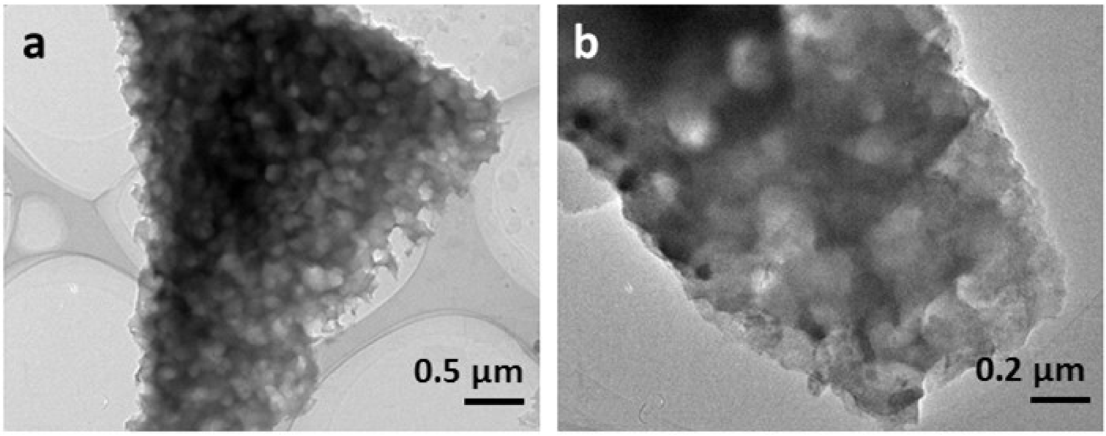

Fig. S1 The TEM images of porous SiO.

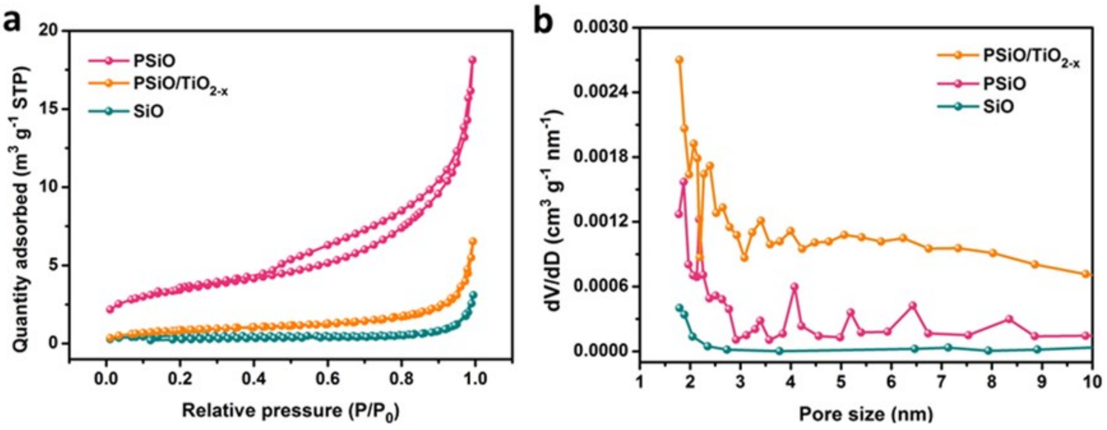

Fig. S2 (a) The Nitrogen adsorption–desorption isotherms and (b) pore size distribution of SiO, porous SiO and porous SiO/TiO_{2-x} composites, respectively.

Table S1 The element content of porous SiO/TiO_{2-x} composites based on XPS measurement.

Element	Si	Ti	O
Content (wt. %)	34.3	12.0	43.8

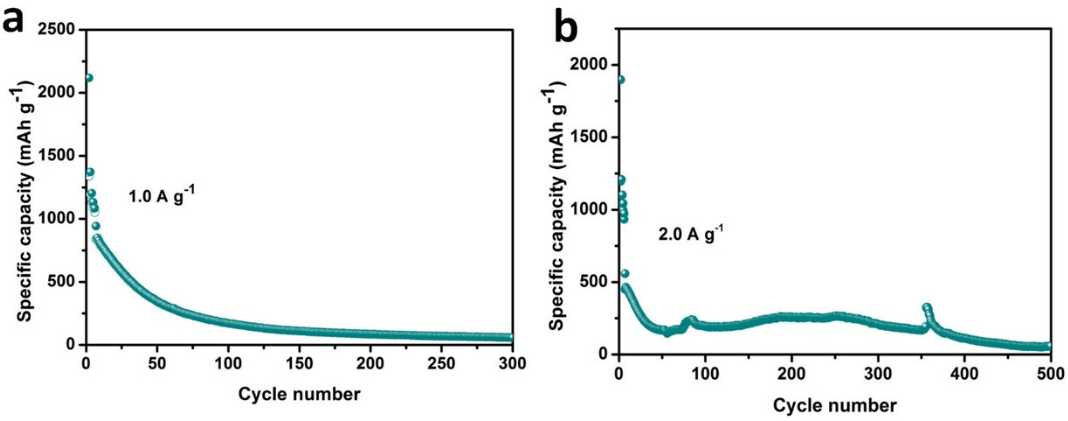

Fig. S3 (a, b) The long-term cycling tests of SiO electrode at 1.0 A g^{-1} and 2.0 A g^{-1}, respectively.

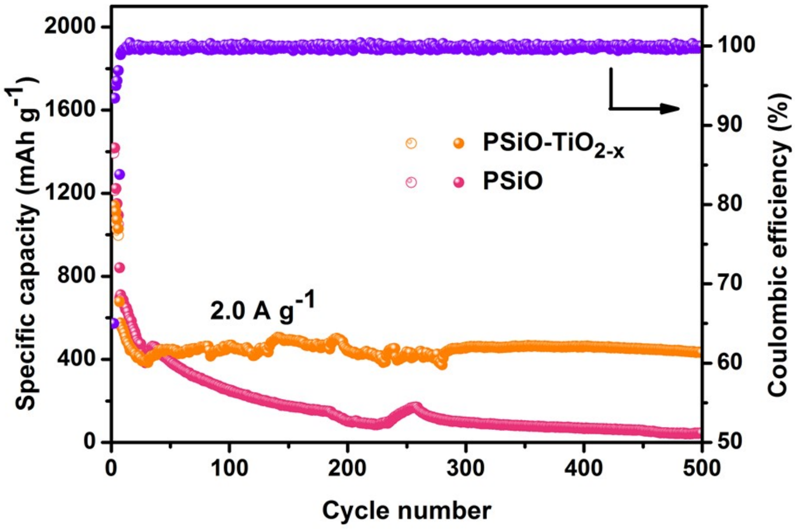

Fig. S4 The long-term cycling tests and the corresponding columbic efficiency of porous SiO/TiO$_{2-x}$ and cycling performance of porous SiO at 2.0 A g^{-1}.

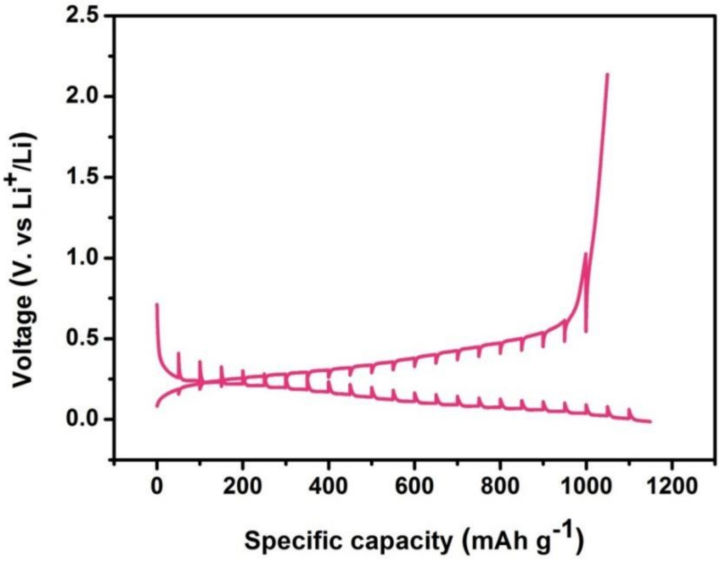

Fig. S5 The GITT curves of porous SiO electrode at the third cycle.

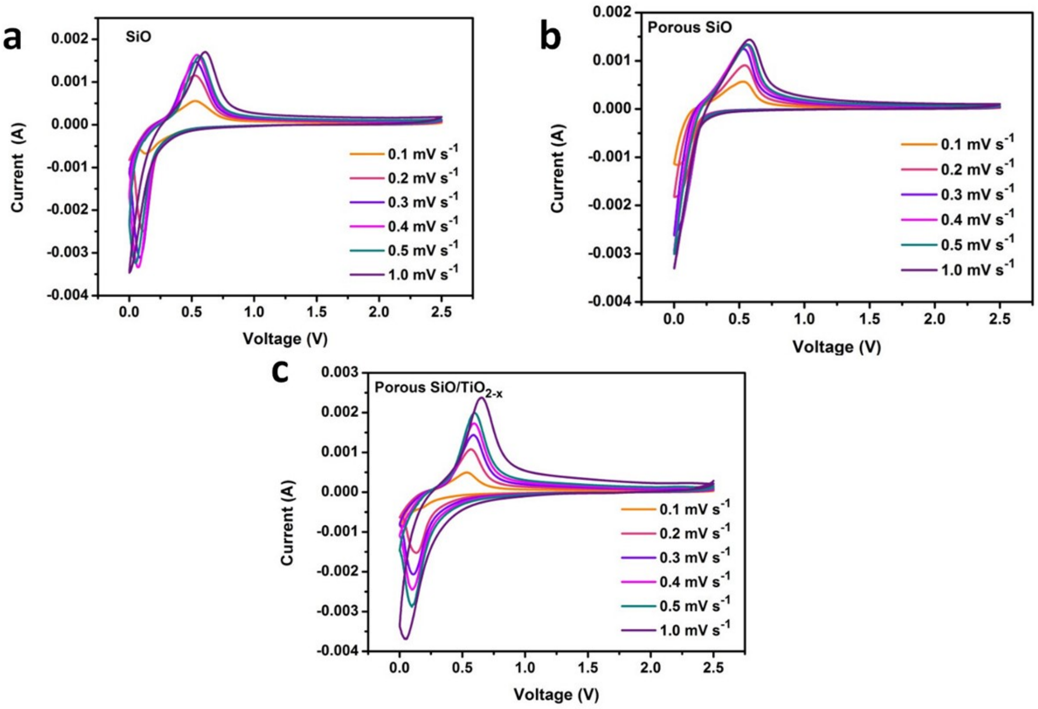

Fig. S6 The CV curves of (a) SiO, (b) porous SiO and (c) porous SiO/TiO$_{2-x}$ composites from the scanning rate of 0.1 mV s^{-1} to 1.0 mV s^{-1}, respectively.

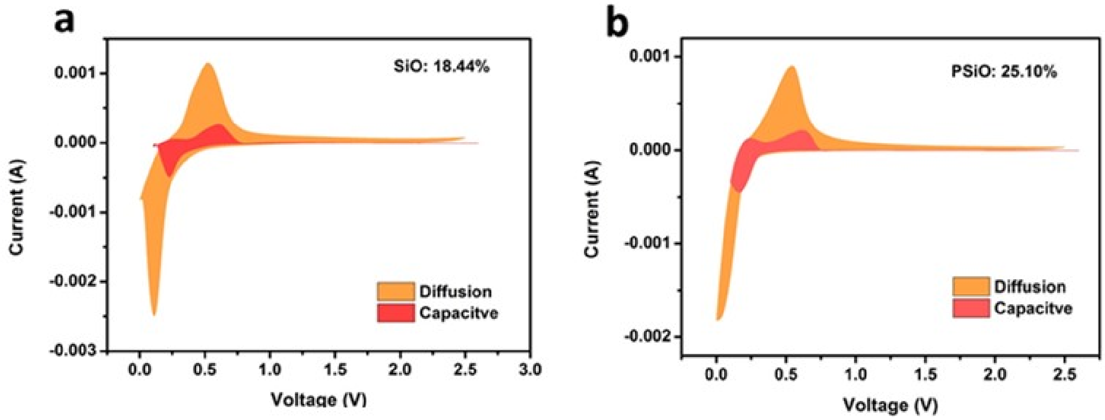

Fig. S7 The capacitive contribution of (a) SiO and (b) porous SiO at the scanning rate of 0.2 mV s^{-1}, respectively.

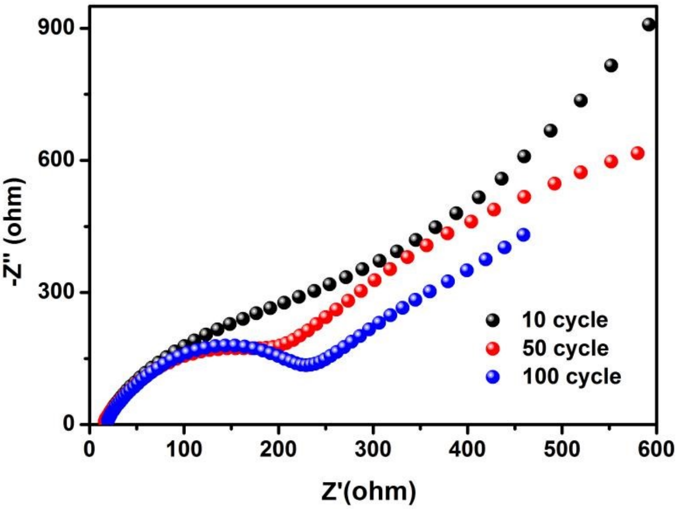

Fig. S8 The Nyquist plots of porous SiO/TiO_{2-x} electrodes obtained after 10, 50 and 100 cycling measurements.

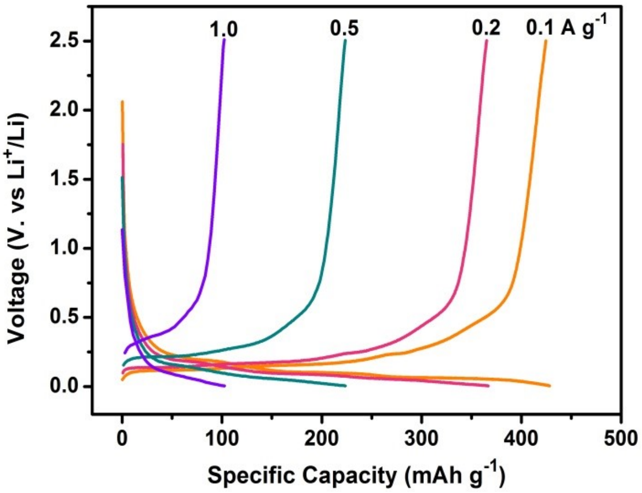

Fig. S9 The charge-discharge curves under various currents of porous SiO/TiO_{2-x} + G.

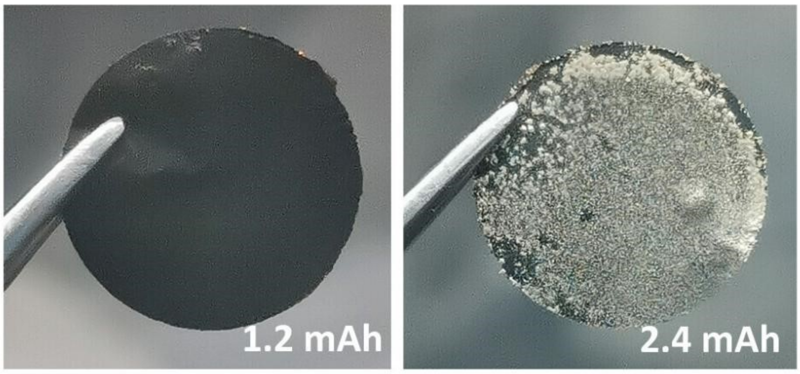

Fig. S10 The optical images of porous SiO electrode taken after Li-metal plating at 1.2 mAh and 2.4 mAh, respectively.